Dynamic and sensor fault tolerant control for an intensified heat-exchanger/reactor

Xue Han, Rim Rammal, Menglin He, Zetao Li, Michel Cabassud, Boutaib Dahhou

Version of Record: https://www.sciencedirect.com/science/article/pii/S0947358022001297
Manuscript_49cb5df42aff0c91572c308cb2642046

Dynamic and sensor fault tolerant control for an intensified heat-exchanger/reactor

Xue Han[a,*], Rim Rammal[a], Menglin He[a,b], Zetao Li[b], Michel Cabassud[c], Boutaib Dahhou[a]

[a] *LAAS-CNRS, Université de Toulouse, CNRS, INSA, UPS,31400 Toulouse, France*
[b] *Electrical Engineering College, Guizhou University, Guiyang 550025, China*
[c] *LGC, Université de Toulouse, CNRS/INP/UPS, 31432 Toulouse, France*

Abstract

In this paper, an active fault tolerant control system is proposed and applied to a new intensified heat exchanger/reactor system. This method consists of an adaptive observer-based fault detection, isolation, and identification scheme and a control law redesign method based on the backstepping approach. The objective of the application of the fault tolerant control system is to ensure the safety and productivity of this intensified heat exchanger/reactor even in the presence of a fault. Both parameter and sensor faults are considered. The effectiveness of the fault tolerant control method based on adaptive observers is validated by simulations on the heat exchanger/reactor system.

Keywords: Fault tolerant control, fault detection and isolation, adaptive observer, backstepping control, intensified heat exchanger/reactor

1. Introduction

Process Intensification (PI), which is currently attracting a lot of interest in the engineering field, especially in chemical and pharmaceutical industries [1, 2, 3], aims to reduce equipment size and energy consumption while improving process efficiency and safety. One of the applications of PI in chemical processes is the intensified continuous heat exchanger (HEX)/reactor, developed in the LGC laboratory (Laboratoire de Genie Chimique). It is a multi-functional device that combines heat exchanger and reactor in one hybrid unit [4]. Thanks to its remarkable thermal and hydrodynamic performances [5], the intensified HEX reactor is a promising way to meet the increasing requirements for safer operating conditions, lower cost, and higher product quality. However, the safety and productivity of the HEX reactor can be strongly influenced by different kinds of faults, such as actuator faults, parameter faults, and sensor faults. For these reasons, the objective of this paper is to introduce an initial work on maintaining the safety and productivity of the considered HEX reactor model, by applying fault detection and isolation (FDI) and fault tolerant control (FTC) methods.

FTC methods, which are widely studied in control theory over the past three decades, allow a system to operate, possibly at a reduced level, rather than shutting down completely when a part of the system fails. For survey papers on FTC, see [6, 7, 8]. Generally, FTC methods are classified into two types: active FTC

*Corresponding author
Email addresses: xue.han@laas.fr (Xue Han), rim.rammal@laas.fr (Rim Rammal), menglin.he@laas.fr (Menglin He), ztli@gzu.edu.cn (Zetao Li), michel.cabassud@ensiacet.fr (Michel Cabassud), boutaib.dahhou@laas.fr (Boutaib Dahhou)

(AFTC) and passive FTC (PFTC) [6]. The PFTC is designed with a fixed controller which is robust to maintain acceptable performance, while the AFTC is based on the online reconfiguration of the controller using the fault information provided by the FDI process. Normally, the passive approach is easier to apply since neither the FDI unit nor the reconfiguration mechanism is needed. However, the active approach is more flexible to deal with different types of faults [9]. The FDI is then an important step for AFTC [10, 11, 12]. It aims to detect the presence of a fault, locate it and determine its type and value. There are a large number of results related to FDI and they are mainly divided into model-based methods [13, 14] and data-driven methods [15, 16]. On one side, model-based methods use the mathematical model of the system to create redundant measurements and then compute the deviation between them and the real measurements. This deviation is defined as a residual signal, and it is considered as a fault indicator. Data-driven methods, on the other side, are based on the knowledge of a wide part of the history of the process.

Among the model-based FDI methods, observer-based approaches have been widely developed in chemical processes. In [17], a review on the use of observers in chemical systems is provided with a guideline to design and choose the appropriate observers for implementation. In [18] and [19], applications of observer-based FDI methods on a continuous stirred tank reactor are presented. For the considered HEX reactor system, its mathematical model has already been developed in [20] and many observer-based FDI methods have been proposed, for example, for the multi-level fault reconstruction [21], actuator fault diagnosis [22], and for integrated actuator, dynamic, and sensor fault diagnosis [23]. However, fault diagnosis is not sufficient for the complete procedure of AFTC. In order to guarantee the safety and productivity of the reactor, a reconfigurable controller should also be designed and reconstructed as soon as the fault is isolated and estimated. In [24], a multiple-model-based FTC scheme has been proposed. Model banks and controller banks are constructed based on the identification of the system and the model predictive control. However, the construction of sub-models and sub-controllers is time-consuming. Therefore, in this paper, we propose a new AFTC system for the HEX reactor.

Recently, in [25], different nonlinear observers have been applied to the HEX system in order to compare them by choosing the convergence speed and the oscillation of the estimation error system as criteria. Simulation results showed that the adaptive observer (AO) has the shortest convergence time and the minimum oscillation. Therefore, the AO is employed in this paper to develop the AFTC strategy. For the purpose of the online fault reconfiguration or the online controller redesign, the backstepping control method, which is a recursive input design procedure, has proven to be reliable and effective in chemical processes. It aims to design a feedback controller while guaranteeing the global asymptotic stability of the system behavior [26]. For example, in [27], a fuzzy adaptive backstepping control has been proposed to make the outputs of a continuous stirred tank reactor follow their reference signals. In [28], a recursive backstepping design approach has been applied to control the temperature and monomer concentration of the polymerization process. Thus, in this paper, a control law based on backstepping theory is constructed for the considered HEX reactor in order to guarantee good performance and the safety of the system. Both parameter faults and sensor faults are considered in this work.

This paper is organized as follows: Section 2 presents the basic mathematical model of the HEX reactor

system, and in Section 3, the control input of the system, in the fault-free case, is constructed using the backstepping method. In Section 4, the AFTC design for the HEX reactor system is presented and its validity is shown by simulations in Section 5. Finally, Section 6 concludes the paper.

2. Modeling of the intensified HEX reactor system

The intensified HEX reactor considered in this paper is represented in Figure 1. The system consists of three process plates, four utility plates, and eight plate walls. All plates are engraved with channels of 2 mm square section. The reactants are injected into the process channels and the reaction takes place here. The water is injected into the utility channels in order to cool or heat the reaction, and the plate walls act as the heat exchange media. In [20], a detailed modeling procedure of the HEX reactor is presented. According to its physical structure, the system is divided into 17 identical units, each unit contains three process channels, four utility channels, and eight plate wall channels.

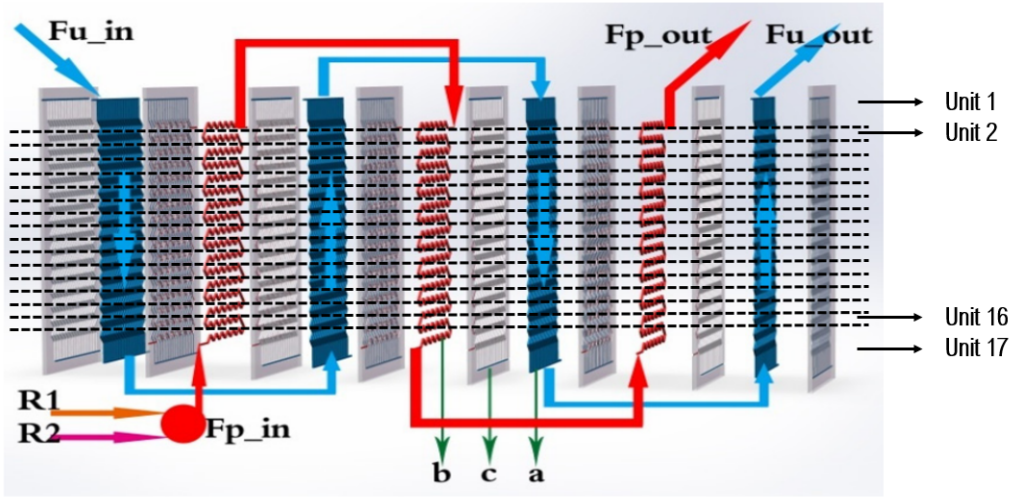

Figure 1: (a) Utility plate; (b) Process plate; (c) Plate wall [20]

In this paper, an AFTC system, which is based on the AO FDI method and the backstepping control law redesign approach, is proposed and applied to the presented HEX reactor model. As a first step, a simplified system with only one unit is considered. The study is divided into two parts: AO-based FTC for the heat exchange procedure without the reaction and AO-based FTC for the heat exchange procedure with the reaction.

For the first study without the reaction, water with different temperatures is injected into the process channel and the utility channel. The system of equations is then given by:

$$\begin{cases} \dot{T}_p = \dfrac{F_p}{V_p}(T_{p,in} - T_p) + \dfrac{h_p A_p}{\rho_p V_p C_{p,p}}(T_w - T_p) \\ \dot{T}_u = \dfrac{F_u}{V_u}(T_{u,in} - T_u) + \dfrac{h_u A_u}{\rho_u V_u C_{p,u}}(T_w - T_u) \\ \dot{T}_w = \dfrac{h_p A_p}{\rho_w V_w C_{p,w}}(T_p - T_w) + \dfrac{h_u A_u}{\rho_w V_w C_{p,w}}(T_u - T_w) \end{cases} \tag{1}$$

where T represents the temperature, F represents the flow rate of the fluid injected into the channels. The subscript p, u, and w represent the process plate, utility plate, and plate wall, respectively. The subscript in is for the inlet fluid. h, A, ρ, V, and C_p are constant parameters for heat transfer coefficient, heat exchange area, density, volume, and specific heat of the material, respectively. The flow rates F_p and F_u are the inputs of the system that control the temperatures. Generally, reactants are injected into the process channel with a fixed flow rate and an optimal proportion to have high productive resultants. Therefore, the only input variable of this system is F_u. In this context, we denote by $x = [T_p \quad T_u \quad T_w]^T$ the state vector of the system and by $u = F_u$ the input variable. The measured output vector is given by $y = x$, *i.e.* the full state vector is measured. The parameter values of the system are given in Table 1.

Table 1: Parameters of the HEX reactor system

Parameter	**Value**	**Units**
h_p	7.5975×10^3	$\mathrm{W \cdot m^{-2} \cdot K^{-1}}$
h_u	7.5833×10^2	$\mathrm{W \cdot m^{-2} \cdot K^{-1}}$
A_p	2.68×10^{-2}	$\mathrm{m^2}$
A_u	4.564×10^{-1}	$\mathrm{m^2}$
$C_{p,p}, C_{p,u}$	4.186×10^3	$\mathrm{J \cdot kg^{-1} \cdot K^{-1}}$
$C_{p,w}$	5×10^2	$\mathrm{J \cdot kg^{-1} \cdot K^{-1}}$
ρ_p, ρ_u	10^3	$\mathrm{kg \cdot m^{-3}}$
ρ_w	8×10^3	$\mathrm{kg \cdot m^{-3}}$
V_p	2.68×10^{-5}	$\mathrm{m^3}$
V_u	1.141×10^{-4}	$\mathrm{m^3}$
V_w	1.355×10^{-3}	$\mathrm{m^3}$

The main application of the HEX reactor is to carry out reactions that involve heat removal or supply issues under concentrated conditions. Therefore, for the second study, an exothermic reaction of the oxidation of sodium thiosulfate by hydrogen peroxide is injected into the process channel:

$$2Na_2S_2O_3 + 4H_2O_2 \rightarrow Na_2S_3O_6 + Na_2SO_4 + 4H_2O \tag{2}$$

The model of the HEX reactor with the consideration of the reaction is given by the following system:

$$\begin{cases} \dot{T}_p &= \dfrac{F_{p,1}+F_{p,2}}{V_p}(T_{p,in}-T_p) + \dfrac{h_pA_p}{\rho_pV_pC_{p,p}}(T_w-T_p) + \dfrac{\Delta H}{\rho_pC_{p,p}}kC_1C_2 \\ \dot{T}_u &= \dfrac{F_u}{V_u}(T_{u,in}-T_u) + \dfrac{h_uA_u}{\rho_uV_uC_{p,u}}(T_w-T_u) \\ \dot{T}_w &= \dfrac{h_pA_p}{\rho_wV_wC_{p,w}}(T_p-T_w) + \dfrac{h_uA_u}{\rho_wV_wC_{p,w}}(T_u-T_w) \\ \dot{C}_1 &= \dfrac{F_{p,1}+F_{p,2}}{V_p}(C_{1,in}-C_1) - 2kC_1C_2 \\ \dot{C}_2 &= \dfrac{F_{p,1}+F_{p,2}}{V_p}(C_{2,in}-C_2) - 4kC_1C_2 \end{cases} \tag{3}$$

where ΔH is the heat coefficient of the reaction, and k is the kinetic constant of the reaction governed by Arrhenius law:

$$k = k_0 exp\Big(- \frac{E^a}{R(T_p + 273.15)}\Big)$$

with k_0 is the pre-exponential factor of the reaction, E^a is the activation energy, and R is the perfect gas constant. Variables C_i for $i = 1, 2$ represents the concentration of reactants $Na_2S_2O_3$ and H_2O_2, respectively. Finally, $C_{1,in}$ and $C_{2,in}$ are the inlet concentration of the first and the second reactant.

Designing an effective control law for the HEX reactor system, described by (1), is very important for the system stability and output regulation. In the next section, the construction of the backstepping-based control law is presented.

3. Backstepping controller design

The backstepping control design is a technique developed in [26] for designing stabilizing controllers for nonlinear systems. The basic idea of the backstepping method is to construct a controller recursively by using some of the state variables as intermediate virtual control signals. In order to guarantee the stability of the entire system, Lyapunov functions are derived recursively [29, 30, 31]. For the HEX reactor (1), the objective is to ensure that the actual temperature of the process fluid T_p follows the desired process temperature $T_{p,d}$, by adjusting the input $u = F_u$. For the system (3) with the reaction, the construction of the control law follows the same following steps.

Consider the HEX reactor model (1). The process temperature error, denoted by e_{T_p}, is defined by the difference between the process temperature T_p and its desired value $T_{p,d}$:

$$e_{T_p} = T_{p,d} - T_p. \tag{4}$$

The dynamic of e_{T_p} is then given by:

$$\begin{aligned} \dot{e}_{T_p} &= \dot{T}_{p,d} - \dot{T}_p \\ &= \dot{T}_{p,d} - \frac{F_p}{V_p}(T_{p,in} - T_p) - \frac{h_p A_p}{\rho_p V_p C_{p,p}}(T_w - T_p). \end{aligned} \tag{5}$$

For the stability analysis, we consider the following Lyapunov function:

$$V_{T_p} = \frac{1}{2} e_{T_p}^2, \tag{6}$$

which is quadratic and positive definite. By deriving (6), we obtain:

$$\dot{V}_{T_p} = e_{T_p}\dot{e}_{T_p} = e_{T_p}(\dot{T}_{p,d} - \frac{F_p}{V_p}(T_{p,in} - T_p) - \frac{h_p A_p}{\rho_p V_p C_{p,p}}(T_w - T_p)) \tag{7}$$

Here, the state T_w, which represents the temperature of the plate wall, is considered as the first virtual controller. In order to make (7) negative definite, the desired temperature $T_{w,d}$ is given by:

$$T_{w,d} = \frac{\rho_p V_p C_{p,p}}{h_p A_p}\left[\dot{T}_{p,d} + k_1 e_{T_p} - \frac{F_p}{V_p}(T_{p,in} - T_p)\right] + T_p, \tag{8}$$

where k_1 is a positive constant. Injecting $T_{w,d}$ into (7) gives:

$$\dot{V}_{T_p} = -k_1 e_{T_p}^2 \leq 0, \tag{9}$$

In the same way, we define by e_{T_w} the error between the temperature T_w and its desired value $T_{w,d}$:

$$e_{T_w} = T_{w,d} - T_w. \tag{10}$$

Its dynamic is given by:

$$\begin{aligned}\dot{e}_{T_w} &= \dot{T}_{w,d} - \dot{T}_w \\ &= \frac{\rho_p V_p C_{p,p}}{h_p A_p}(\ddot{T}_{p,d} + k_1 \dot{e}_{T_p} + \frac{F_p}{V_p}\dot{T}_p) + \dot{T}_p - \frac{h_p A_p}{\rho_w V_w C_{p,w}}(T_p - T_w) - \frac{h_u A_u}{\rho_w V_w C_{p,w}}(T_u - T_w).\end{aligned} \tag{11}$$

In order to guarantee the stability of e_{T_w}, we consider the following Lyapunov function:

$$\begin{aligned}V_{T_w} &= \frac{1}{2}e_{T_p}^2 + \frac{1}{2}e_{T_w}^2 \\ &= V_{T_p} + \frac{1}{2}e_{T_w}^2\end{aligned} \tag{12}$$

with dynamic given by:

$$\dot{V}_{T_w} = \dot{V}_{T_p} + e_{T_w}\dot{e}_{T_w}. \tag{13}$$

where $\dot{V}_{T_p}$ and $\dot{e}_{T_w}$ are given by (9) and (11), respectively.

Once again, the state T_u is considered as a second virtual controller with the desired value $T_{u,d}$ given by:

$$\begin{aligned}T_{u,d} =& \frac{\rho_w V_w C_{p,w}}{h_u A_u}\left[\frac{h_p A_p}{\rho_p V_p C_{p,p}} e_{T_p} + \frac{\rho_p V_p C_{p,p}}{h_p A_p}(\ddot{T}_{p,d} + k_1\dot{e}_{T_p} + \frac{F_p}{V_p}\dot{T}_p) + \dot{T}_p\right. \\ & \left. - \frac{h_p A_p}{\rho_w V_w C_{p,w}}(T_p - T_w) + k_2 e_{T_w}\right] + T_w,\end{aligned} \tag{14}$$

where k_2 is a positive constant. Injecting $T_{u,d}$ in (13) yields to:

$$\dot{V}_{T_w} = -k_1 e_{T_p}^2 - k_2 e_{T_w}^2 \leq 0 \tag{15}$$

hence, the stability of the error e_{T_w} is ensured.

Finally, in order to get the expression of the controller F_u, an error e_{T_u} is defined by:

$$e_{T_u} = T_{u,d} - T_u \tag{16}$$

and its dynamic is given by:

$$\dot{e}_{T_u} = \dot{T}_{u,d} - \dot{T}_u. \tag{17}$$

We consider the following Lyapunov function:

$$\begin{aligned}V_{T_u} =& \frac{1}{2}e_{T_p}^2 + \frac{1}{2}e_{T_w}^2 + \frac{1}{2}e_{T_u}^2 \\ =& V_{T_w} + \frac{1}{2}e_{T_u}^2,\end{aligned} \tag{18}$$

with

$$\dot{V}_{T_u} = \dot{V}_{T_w} + e_{T_u}\dot{e}_{T_u}. \tag{19}$$

Finally, the control law F_u is given by:

$$\begin{aligned}F_u =& \frac{V_u}{T_{u,in} - T_u}\left\{\frac{h_u A_u}{\rho_w V_w C_{p,w}} e_{T_w} + \frac{\rho_w V_w C_{p,w}}{h_u A_u}\left[\frac{h_p A_p}{\rho_p V_p C_{p,p}}\dot{e}_{T_p} + \frac{\rho_p V_p C_{p,p}}{h_p A_p}(\dddot{T}_{p,d} + k_1\ddot{e}_{T_p} + \frac{F_p}{V_p}\ddot{T}_p)\right.\right. \\ & \left. + \ddot{T}_p - \frac{h_p A_p}{\rho_w V_w C_{p,w}}(\dot{T}_p - \dot{T}_w) + k_2\dot{e}_{T_w}\right] + \frac{h_p A_p}{\rho_w V_w C_{p,w}}(T_p - T_w) + \frac{h_u A_u}{\rho_w V_w C_{p,w}}(T_u - T_w) \\ & \left. - \frac{h_u A_u}{\rho_u V_u C_{p,u}}(T_w - T_u) + k_3 e_{T_u}\right\}\end{aligned}, \tag{20}$$

where k_3 is a positive constant. Consequently, substituting (17) and (20) into (19) yields to:

$$\dot{V}_{T_u} = -k_1 e_{T_p}^2 - k_2 e_{T_w}^2 - k_3 e_{T_u}^2 \leq 0 \tag{21}$$

Thus, the closed-loop system is globally asymptotically stable.

The effectiveness of the backstepping controller on the HEX reactor model is validated by simulations, see Figure 2. Water with different temperatures and flow rates is injected into the process channel and utility channel. For the process channel, $T_{p,in} = 77$ °C and $F_p = 10$ L $\cdot$ h^{-1}, and for the utility channel, $T_{u,in} = 15.6$ °C and $F_u = 62.2$ L $\cdot$ h^{-1}. Initial temperatures of the state vector in (1) are $[T_p \quad T_u \quad T_w]^T = [77 \quad 15.6 \quad 15.6]^T$. Initially, the desired temperature $T_{p,d}$ is settled at 27 °C and then at 400 s it passes to 25 °C. Using the reference trajectory of $T_{p,d}$ and the backstepping technique, the control law F_u is calculated by (20). As shown in Figure 2, the measured temperature of the process fluid T_p follows the desired temperature $T_{p,d}$.

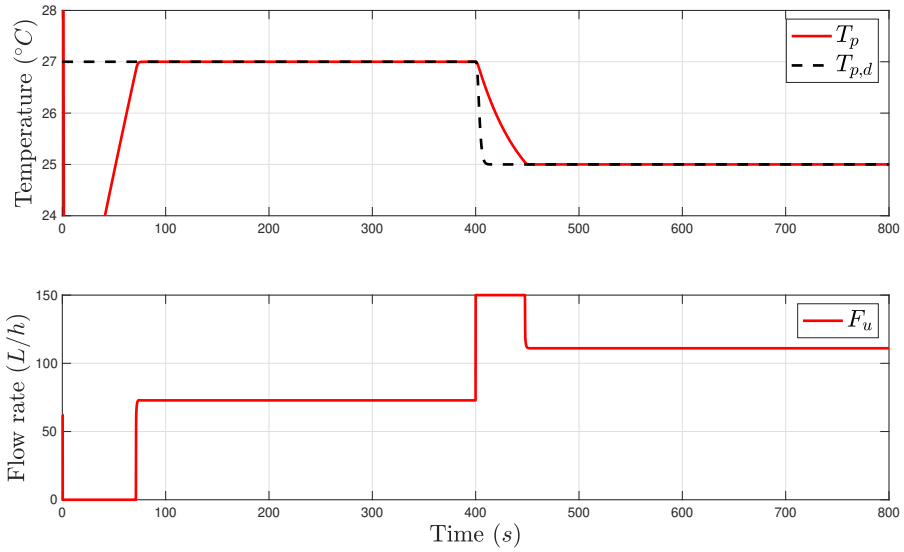

Figure 2: Temperature of process fluid T_p and flow rate of utility fluid F_u in the fault free case.

The HEX reactor system, considered in this paper, is a high intensified device, so it cannot be opened for cleaning once the assembly is finished. Therefore, in the presence of faults on the system sensors or parameters, an AFTC technique can be applied to the system (1), which is the aim of the next section.

4. AFTC for the HEX reactor system

4.1. Problem statement

In reality, for the HEX reactor model, both process channels and utility channels could be fouled, and then, the heat exchange performance will gradually decline. Therefore, it is necessary to supervise the dynamics of fouling. For the proposed HEX reactor, the fouling in both channels will result in the decrease of heat transfer coefficients h_p and h_u [23, 24]. In addition, the temperature of both inlet fluids $T_{p,in}$ and $T_{u,in}$ could be affected by sudden environmental change or unexpected malfunction of the thermocouples in

the pipes [24]. However, since the chemical reaction takes place in the process channels, the parameters h_p and $T_{p,in}$ are more subject to faults than the h_u and $T_{u,in}$ parameters. Moreover, sensors are devices that can be subject to malfunctions: they can represent gain losses or extra biases. The presence of these kinds of faults may cause serious damage to the system and may affect productivity. For this purpose, we propose to apply an AFTC method to the HEX reactor model.

As shown in Figure 3, the proposed AFTC system is composed of two steps, an FDI scheme, and a controller reconfiguration mechanism. Therefore, the fault is firstly detected, isolated, and identified, and then the control law is redesigned using the fault information. As presented in Section 1, we use AOs for FDI and the backstepping controller redesign method for control law reconfiguration. In the AO-based FDI method, a bank of N observers is constructed to deal with N possible faults. In this section, the AFTC scheme based on AO is represented for the system (1) without the reaction. For the system (3), the procedure is the same.

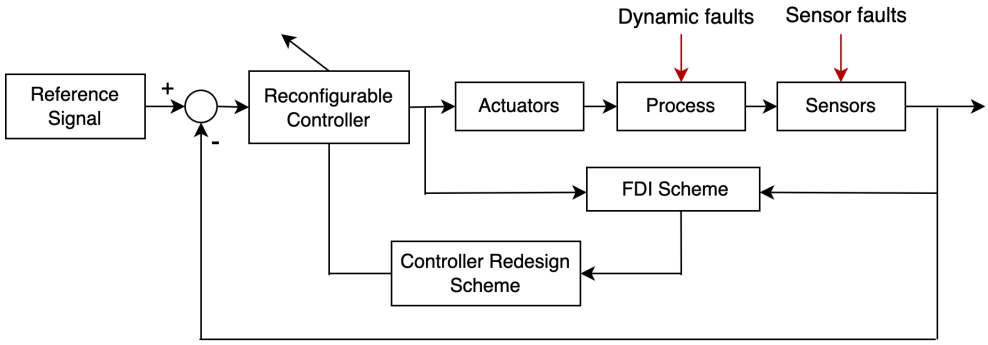

Figure 3: General structure of the proposed AFTC system.

4.2. Modeling of the faulty HEX reactor system

The HEX reactor system (1) can be written into the general nonlinear form:

$$\begin{cases} \dot{x} = f(x) + g(x)u + p(x)\beta \\ y = Cx \end{cases} \tag{22}$$

where x is an n-dimensional state vector, u is an m-dimensional input vector, y is a q-dimensional output vector, and β is the possible faulty parameter vector of dimension k. $f(x) \in \mathbf{R}^{n\times 1}$, $g(x) \in \mathbf{R}^{n\times m}$ and $p(x) \in \mathbf{R}^{n\times k}$ are matrices of nonlinear functions, and $C \in \mathbf{R}^{q\times n}$ is the output matrix. We recall that for the HEX reactor model (1), $x = y = [T_p \quad T_u \quad T_w]^T$, $u = F_u$ and $\beta = [h_p \quad T_{p,in}]^T$, therefore, $n = 3$, $m = 1$, $q = 3$ and $k = 2$. The function matrices are given by:

$$f(x) = \begin{pmatrix} -\dfrac{F_p}{V_p}T_p \\ \dfrac{h_u A_u}{\rho_u V_u C_{p,u}}(T_w - T_u) \\ \dfrac{h_u A_u}{\rho_w V_w C_{p,w}}(T_u - T_w) \end{pmatrix}, \quad g(x) = \begin{pmatrix} 0 \\ \dfrac{T_{u,in} - T_u}{V_u} \\ 0 \end{pmatrix}, \quad p(x) = \begin{pmatrix} \dfrac{A_p}{\rho_p V_p C_{p,p}}(T_w - T_p) & \dfrac{F_p}{V_p} \\ 0 & 0 \\ \dfrac{A_p}{\rho_w V_w C_{p,w}}(T_p - T_w) & 0 \end{pmatrix}, \tag{23}$$

respectively and the output matrix $C = I_3$ is the identity matrix of dimension 3.

A parameter fault refers to variations in a process parameter β_j of the parameter vector β, and we denote by f_p the vector of the possible parameter faults. If, at a time t_f, a fault occurs on the j^{th} parameter, then, for all $t \geqslant t_f$, the faulty parameter, denoted by $\beta_j^f(t)$, is given by:

$$\beta_j^f(t) = \beta_j(t) + f_{pj} \tag{24}$$

where f_{pj} is the j^{th} element of the vector f_p. In this case, the HEX reactor model (22) can be written into the following parameter faulty model:

$$\begin{cases} \dot{x} = f(x) + g(x)u + \sum\limits_{\substack{i=1 \\ i \neq j}}^{k} p_i(x)\beta_i + p_j(x)\beta_j^f \\ \\ y = Cx \end{cases} \tag{25}$$

where $p_l(x) = [p_{1,l}(x) \quad \dots \quad p_{n,l}(x)]^T$ is the l^{th} column of the matrix $p(x)$.

A sensor fault can be modeled in the same way as the parameter fault. We denote by f_s the vector of possible sensor faults. If, at a time t_f, a fault appears on the j^{th} sensor, then for all $t \geqslant t_f$, the faulty output, denoted by $y_j^f(t)$, is expressed by:

$$y_j^f(t) = y_j(t) + f_{sj} \tag{26}$$

where f_{sj} is the j^{th} element of the vector f_s. In this case, the HEX reactor system (22) becomes:

$$\begin{cases} \dot{x} = f(x) + g(x)u + p(x)\beta \\ y_i = C_i\, x, \qquad \text{for } \; i = 1, \dots, q, \quad i \neq j \\ y_j^f = C_j\, x + f_{sj} \end{cases} \tag{27}$$

where C_i is the i^{th} row of the output matrix C. In the HEX reactor system, both fault vectors f_p and f_s are limited signals, *i.e.* $\|f_p\| \leqslant M_p$, and $\|f_s\| \leqslant M_s$ (M_p and M_s are positive known constants).

4.3. Adaptive observers design for faulty systems

In order to detect, isolate, and identify faults on the system parameters, using the AO-based method, a bank of k AOs, corresponding to the k parameters, is constructed for the faulty model (25):

$$1 \leq j \leq k \quad \begin{cases} \dot{\hat{x}}^{(j)} = f(x) + g(x)u + \sum\limits_{\substack{i=1 \\ i \neq j}}^{k} p_i(x)\beta_i + p_j(x)\hat{\beta}_j^f + H_j(\hat{x}^{(j)} - x) \\ \\ \dot{\hat{\beta}}_j^f = -2\gamma_j(\hat{x}^{(j)} - x)^T S_j p_i(x) \\ \hat{y}^{(j)} = C\hat{x}^{(j)} \end{cases} \tag{28}$$

where $\hat{x}^{(j)}$ is the estimated state vector by the j^{th} AO, $\hat{\beta}_j^f$ is the estimation of the faulty parameter β_j^f and $\hat{y}^{(j)}$ is the estimated output vector. The matrix H_j is a Hurwitz matrix, γ_j is a design parameter, and S_j is a positive definite matrix obtained by:

$$H_j^T S_j + S_j H_j = -Q_j \tag{29}$$

where Q_j is a positive definite matrix that can be chosen freely.

Similarly, for the case of sensor faults, a bank of q observers, corresponding to the q available sensors, are constructed for the faulty model (27):

$$1 \leq j \leq q \quad \begin{cases} \dot{\hat{x}}^{(j)} = f(x) + g(x)u + p(x)\beta + H_j(\hat{x}^{(j)} - x) \\ \hat{y}^{(j)} = \left[C_1\hat{x}^{(j)} \quad ... \quad \hat{y}_j^{(j)^f} \quad ... \quad C_q\hat{x}^{(j)} \right]^T \\ \dot{\hat{y}}_j^{(j)^f} = -2\gamma_j(\hat{x}^{(j)} - x)^T S_j C_j^T \end{cases} \tag{30}$$

where C_i is the i^{th} row of the output matrix C and $\hat{y}_j^{(j)^f}$ is the estimation of the faulty sensor using the j^{th} observer. The matrices H_i and S_i and the constant γ_i are chosen as the same manners as that in dynamic fault case (see eq (29)).

4.4. FDI and fault reconfiguration

In order to detect and identify a dynamic or a sensor fault on the system, residual signals are generated by the difference between the system output y and the output of the i^{th} observer $\hat{y}^{(i)}$. For example, in the case of parameter faults, we have m different residuals given by:

$$r_i = \|\hat{y}^{(i)} - y\|, \quad i \in 1, \ldots, m. \tag{31}$$

These residuals are designed to be insensitive to the fault of a particular parameter while being sensitive to others, *i.e.* if the i^{th} parameter is faulty, then the i^{th} residual will converge to zero while the rest $m-1$ residuals stay at a nonzero constant. However, in closed-loop system, the adjustment of the input signal may also cause the variation of these residuals, and that makes it difficult to isolate the fault. To solve it, auxiliary residuals calculated by (32) are used in our fault isolation procedure:

$$Dr_i = \frac{d\|\hat{y}^{(i)} - y\|}{dt}, \quad i \in 1, \ldots, m. \tag{32}$$

When the original residuals r_i, for $i = 1, \ldots, m$, leave zero, it indicates the detection of a change in the system behavior. This variation can be caused by an input change or the occurrence of a fault. In order to identify the reason for this change and avoid false alarms, an analysis of the stability of each residual r_i is performed using the auxiliary residuals Dr_i. Once the original residuals r_i are stable (*i.e.* the corresponding Dr_i are equal to zero), a decision can be made: if all the original residuals are equal to zero, then the residual change is caused by the adjustment of the input signal. However, if only one original residual returns to zero while others converge to a nonzero value, then a fault is detected and isolated on the parameter corresponding to the nonzero residual.

Finally, after detecting and isolating the fault on the j^{th} parameter, an estimation of the fault can be obtained as follows:

$$\hat{f}_{pj} = \hat{\beta}_j^f - \beta_j. \tag{33}$$

This fault information is then used to reconstruct the control F_u of the system using the backstepping technique, represented in Section 3. The nominal backstepping control law F_u given by (20), can be expressed by:

$$F_u = \varphi(T_{p,d}, y, \beta_j, k). \tag{34}$$

The new control law, after the parameter fault, is redesigned using the estimated faulty value, and then given by:

$$F_u = \varphi(T_{p,d}, y, \beta_j + \hat{f}_{pj}, k) \tag{35}$$

The fault on the j^{th} parameter is then compensated.

In the same way, a fault on the j^{th} sensor is detected, isolated, and identified, and the obtained fault estimation is employed to reconstruct the input control F_u, only this time, the new control is given by:

$$F_u = \varphi(T_{p,d}, y_j^f - \hat{f}_{sj}, \beta, k) \tag{36}$$

where $\hat{f}_{sj}$ is the sensor fault estimation.

In the next section, the present AO-based FTC scheme is applied by simulations to the HEX reactor system.

5. Simulation results and discussion

In order to validate the effectiveness of the AO-based FTC scheme on the HEX reactor, simulations were performed for the two studies, with and without the reaction. In these simulations, parameter faults and sensor faults are considered, separately. Our aim is to make the measured temperature of the process fluid T_p follow the desired temperature $T_{p,d}$ even in the presence of parameter or sensor faults.

5.1. Simulation results of the HEX reactor without the reaction

In this section, the AO-based FTC scheme is applied to a simplified HEX reactor model (1) which considers only the heat exchange procedure. The possible parameter faults and sensor faults have been introduced in Section 4. Therefore, we will present simulations when a fault occurs on the heat transfer coefficient h_p, the inlet fluid temperatures $T_{p,in}$, and the first sensor T_p. To deal with the dynamic fault, two AOs are constructed, corresponding to h_p and $T_{p,in}$, and then we have two residuals r_1 and r_2, corresponding to h_p and $T_{p,in}$, respectively. Similarly, two AOs are designed for the possible faulty sensors T_p and T_u. The parameter values of the HEX reactor and the initial values of the temperatures used in these simulations are the same as presented in Section 3.

5.1.1. Dynamic fault on h_p

The nominal value of h_p is 7.5975×10^3 $\text{W} \cdot \text{m}^{-2} \cdot \text{K}^{-1}$. We suppose that the process channel is fouled at $t_f = 200\,\text{s}$, which causes a 15% decrease in the heat transfer coefficient h_p: $f_{p1} = -0.15 \times h_p = -1.1393 \times 10^3$ $\text{W} \cdot \text{m}^{-2} \cdot \text{K}^{-1}$. Then, we get the faulty heat transfer coefficient: $h_p^f = h_p + f_{p1} = 6.4852 \times 10^3$ $\text{W} \cdot \text{m}^{-2} \cdot \text{K}^{-1}$.

Figure 4 shows the performances of the residuals used for FDI. At about $t = 70\,\text{s}$, the original residuals r_i as well as the auxiliary residuals Dr_i change. After the stability of the original residuals, *i.e.* $Dr_i = 0$, for $i = 1, 2$, their values converge to zero, thus this unexpected variation is caused by an adjustment of the input signal F_u and there is no fault at this time. At $t = 200\,\text{s}$, the residuals r_i change again. After about 12 s, the auxiliary residuals become stable, and the first original residual r_1, which relates to the first

observer, returns to zero while the other residual r_2 stays at a nonzero value. Therefore, according to the AO-based FDI, presented in Section 4, a fault is detected and isolated on h_p. The estimated faulty value $\hat{f}_{p1}$ is presented in Figure 5, and it is equal to the given faulty value f_{p1}.

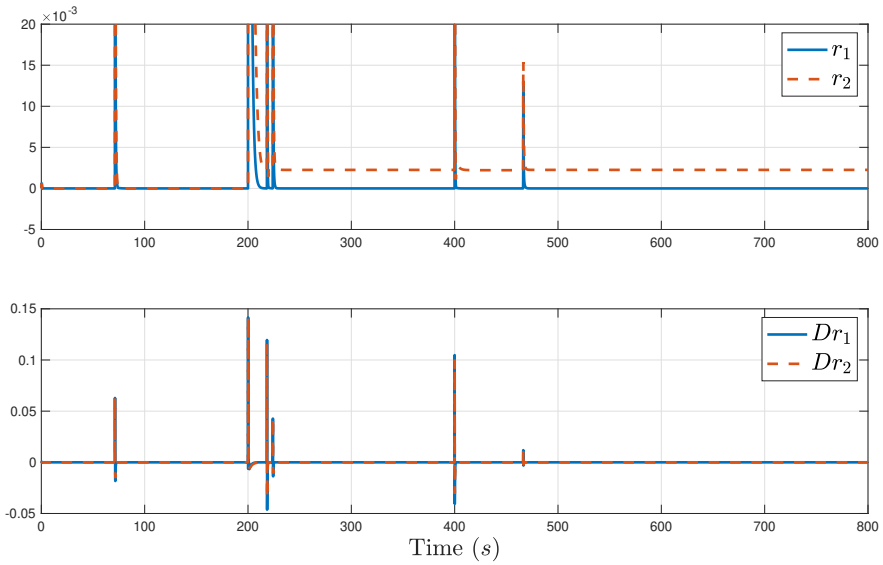

Figure 4: Original residual r_i and auxiliary residual Dr_i when h_p is faulty at $t_f = 200\,\text{s}$.

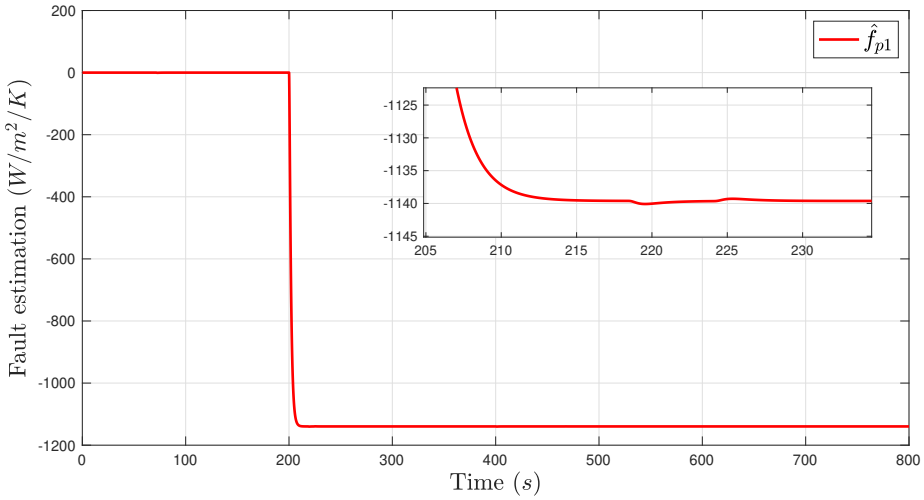

Figure 5: Estimation of the faulty value $\hat{f}_{p1}$ when h_p is faulty at $t_f = 200\,\text{s}$.

Figure 6 represents the behavior of the system after a fault occurs on h_p, when the AO-based FTC is applied (red line) and when it is not (blue dashed line). When the fault occurs at $t_f = 200\,\text{s}$, it is obvious that the measured process fluid temperature T_p is affected. In the absence of the AO-based FTC system, the process fluid temperature T_p cannot follow the expected value $T_{p,d}$ even if the input signal F_u changes to control the system. On the contrary, when the AO-based FTC is applied to the system, the fault on h_p is compensated, and the temperature T_p follows its desired value $T_{p,d}$.

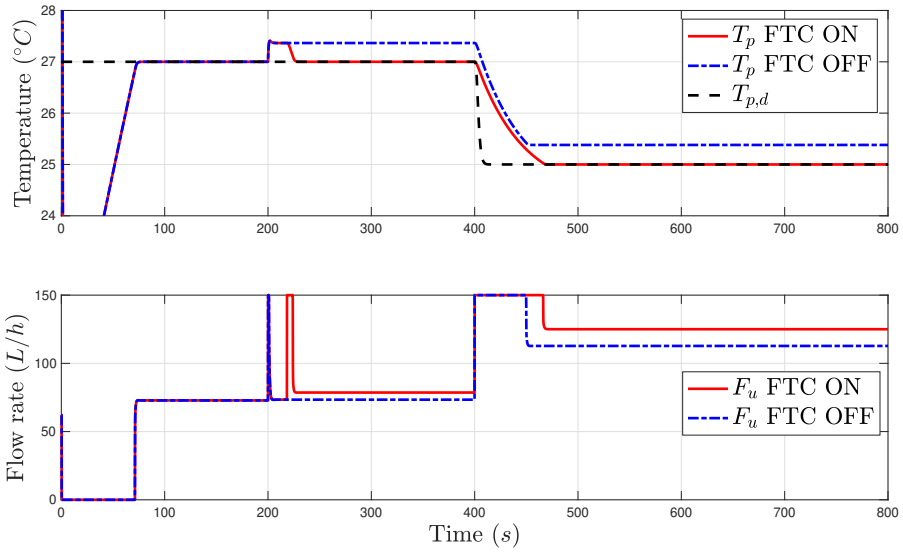

Figure 6: Behavior of the system when a fault occurs on h_p, with and without the AO-based FTC.

5.1.2. Dynamic fault on $T_{p,in}$

We suppose that at $t_f = 200\,\text{s}$, the inlet temperature of the process fluid $T_{p,in}$ changes due to a malfunction in the thermocouples or some environmental changes. Then, the value of $T_{p,in}$ drops from its nominal value $T_{p,in} = 77\,^\circ\text{C}$ to its faulty value $T^f_{p,in} = T_{p,in} + f_{p2} = 72\,^\circ\text{C}$, with $f_{p2} = -5\,^\circ\text{C}$.

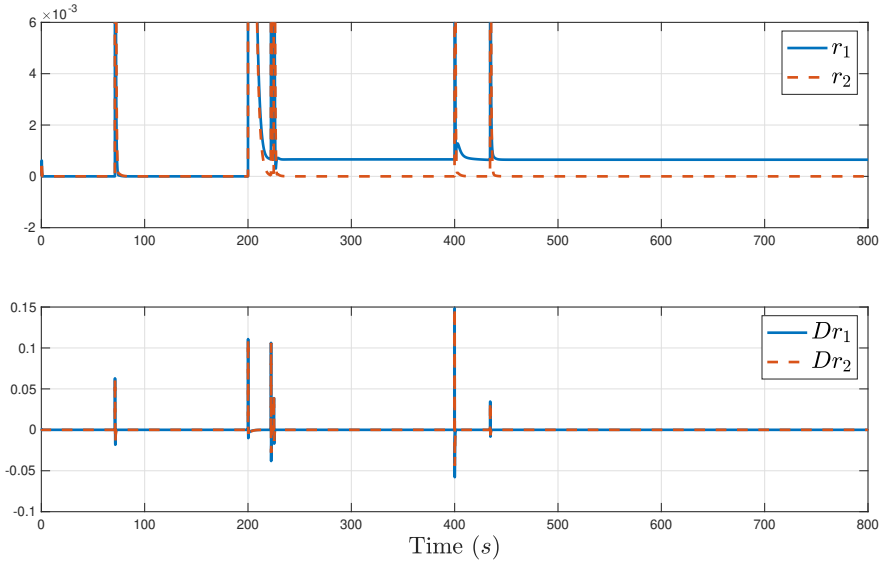

Figure 7: Original residual r_i and auxiliary residual Dr_i when $T_{p,in}$ is faulty at $t_f = 200\,\text{s}$.

Figure 7 shows the residuals used for the AO-based FDI process. The adjustment of the input F_u appears in the change of residuals at about $t = 70\,\text{s}$, since both original residuals are equal to zero when they are stable. However, at $t = 200\,\text{s}$, the original residuals r_i leave zero, and once they are stable, *i.e.* $Dr_i = 0$, $i = 1, 2$, the residual r_2 returns to zero while the residual r_1 convergences to a nonzero value. Thus, the fault is detected

and isolated at $T_{p,in}$, and the fault value $\hat{f}_{p2}$ is estimated. The estimation of the fault value is consistent with the introduced fault value f_{p2}, see Figure 8.

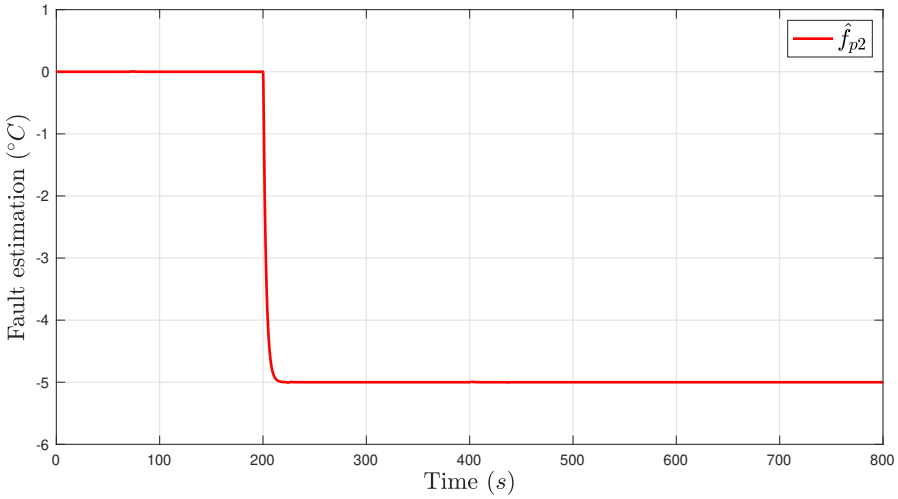

Figure 8: Estimation of the fault value $\hat{f}_{p2}$ when $T_{p,in}$ is faulty at $t_f = 200\,\text{s}$.

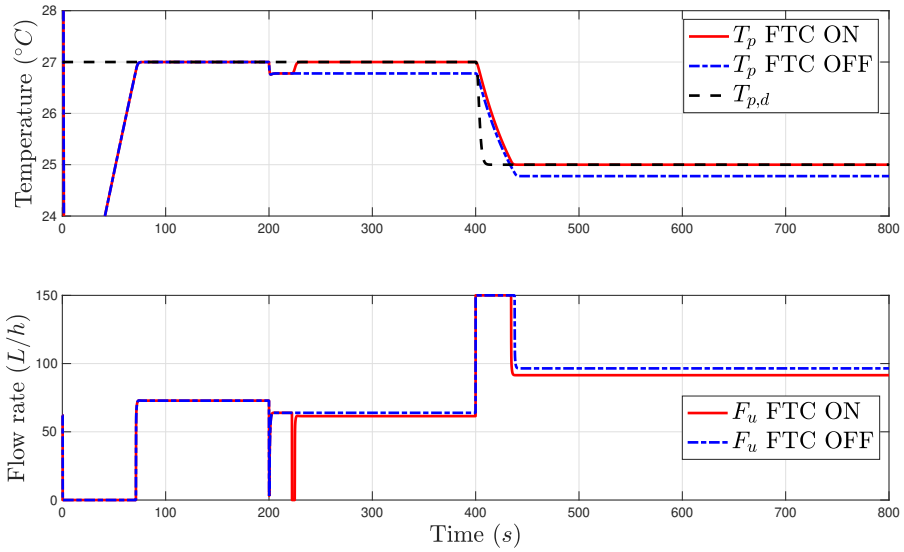

Figure 9: Behavior of the system when a fault occurs on $T_{p,in}$, with and without the AO-based FTC.

Figure 9 shows the difference in the behavior of the HEX reactor when the AO-based FTC system is applied (the red line) and when it is not (the blue dashed line). The AO-based FTC guarantees that the process temperature T_p follows its desired value $T_{p,d}$ even in the presence of a fault on the parameter $T_{p,in}$.

5.1.3. Sensor fault on T_p

In this section, we consider a temperature sensor fault $f_{s1} = -3\,^\circ\text{C}$ that occurs on the first sensor s_1, corresponding to T_p, at $t_f = 200\,\text{s}$. Then, the output of the faulty sensor is $y_1^f = y_1 + f_{s1}$.

The residuals used for the AO-based FDI are illustrated in Figure 10. At $t_f = 200\,\text{s}$, both original residuals r_1 and r_2 leave zero, and once they are both stable ($Dr_i = 0$, $i = 1, 2$) the residual r_1 goes back to zero, and the residual r_2 stays at a nonzero value. Then, according to the AO-based FDI, a fault is detected and isolated on the first sensor. The estimated faulty value $\hat{f}_{s1}$ is also computed and given in Figure 11. Its value is equal to the faulty value f_{s1}.

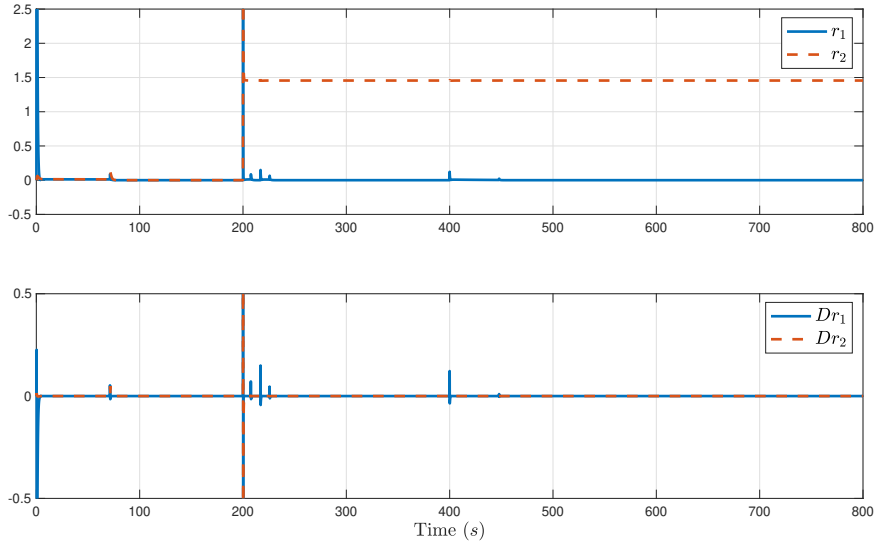

Figure 10: Original residual r_i and auxiliary residual Dr_i when the sensor of T_p is faulty at $t_f = 200\,\text{s}$.

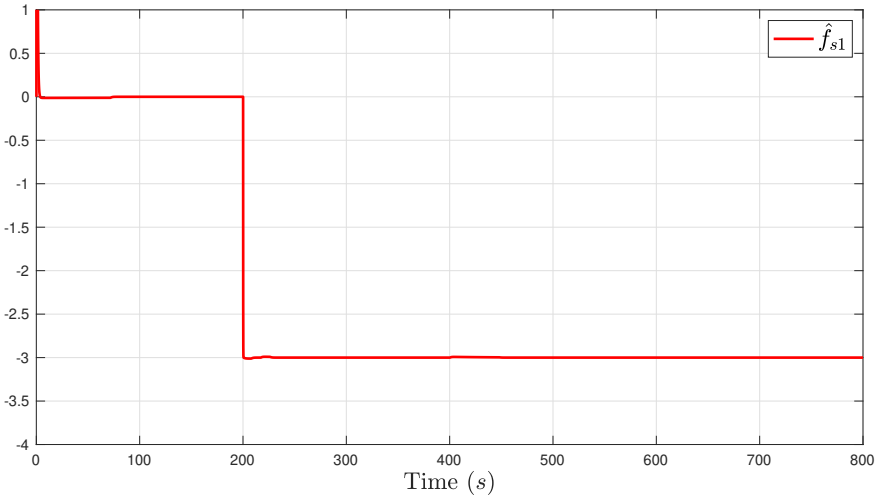

Figure 11: Estimation of the fault value $\hat{f}_{s1}$ when the sensor of T_p is faulty at $t_f = 200\,\text{s}$.

Finally, the obtained fault information is used to compensate the faulty sensor. Figure 12 and Figure 13 present the behavior of the system after the fault when the AO-based FTC system is applied and when it is not, respectively. We can see that when the AO-based FTC is activated, the output of the system (blue dashed line) follows the desired value even if the sensor is faulty (red line). Contrariwise, without the AO-based FTC, the output of the system cannot follow the desired value.

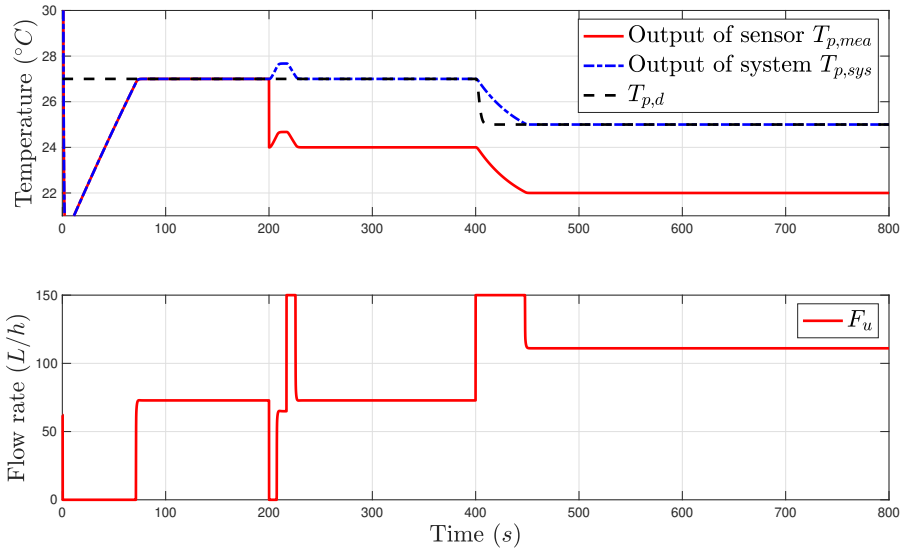

Figure 12: Behavior of the system when a fault occurs on the sensor of T_p, with the AO-based FTC.

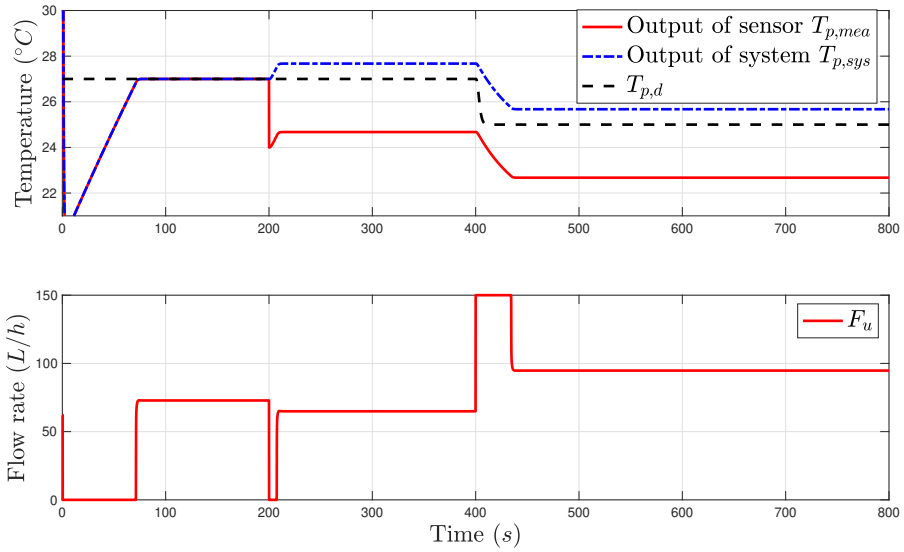

Figure 13: Behavior of the system when a fault occurs on the sensor of T_p, without the AO-based FTC.

5.2. Simulation results of the HEX reactor with chemical reaction

In the following subsections, the AO-based FTC scheme is applied to the HEX reactor with the consideration of reaction. The faulty parameters and faulty sensors considered in this section are the same as those in the former part. In these simulations, reactants are injected into the process channel with the same temperature, $T_{p,in} = 21.1\,^\circ\mathrm{C}$, but with different flow rates, $F_{p,1} = 4.7\ \mathrm{L}\cdot\mathrm{h}^{-1}$, $F_{p,2} = 2.3\ \mathrm{L}\cdot\mathrm{h}^{-1}$. The concentrations are both set to 9% in mass. Water is injected into the utility channel with a temperature $T_{u,in} = 59.4\,^\circ\mathrm{C}$ and a flow rate $F_u = 112.5\ \mathrm{L}\cdot\mathrm{h}^{-1}$. Initial temperatures are $[T_p \quad T_u \quad T_w]^T = [21.1 \quad 59.4 \quad 59.4]^T$. The desired temperature $T_{p,d}$ is settled at $56\,^\circ\mathrm{C}$ at the beginning, and then is changed to $57\,^\circ\mathrm{C}$ after 400 s.

5.2.1. Dynamic fault on h_p

Assume that a decrease of heat transfer coefficient h_p occurs at $t_f = 200\,\text{s}$ due to the fouling in the process channel. The fault value $f_{p1} = -0.2 \times h_p = -1.5195 \times 10^3\ \text{W} \cdot \text{m}^{-2} \cdot \text{K}^{-1}$. Then, we get the faulty heat transfer coefficient: $h_p^f = h_p + f_{p1} = 6.078 \times 10^3\ \text{W} \cdot \text{m}^{-2} \cdot \text{K}^{-1}$.

Different performances of the process fluid temperature T_p (with and without FTC) and the input signal F_u are presented in Figure 14. Before the occurrence of the fault, the desired temperature $T_{p,d}$ is well tracked. At 200 s, the temperature of process fluid T_p changes, and it cannot follow the reference signal. Then, with the help of the FTC method, the process fluid temperature T_p can follow the desired value once the fault is isolated and estimated.

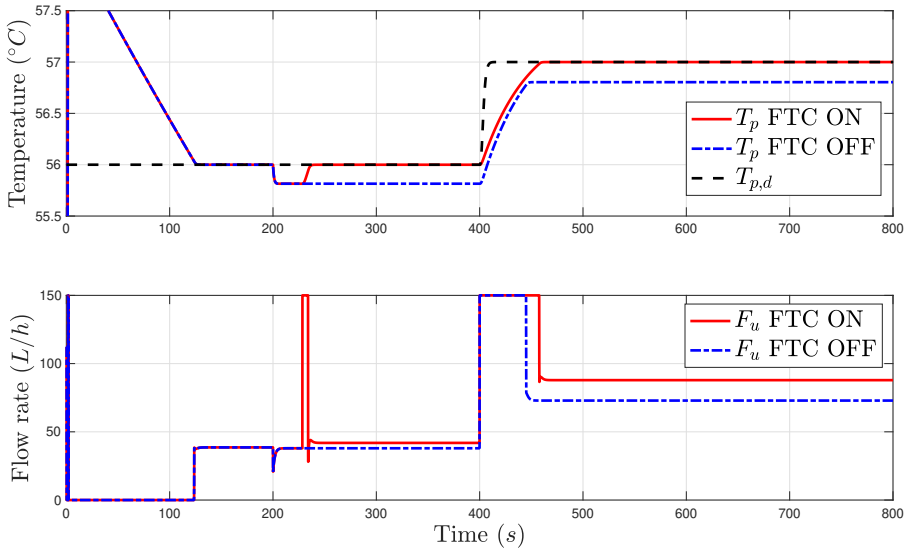

Figure 14: Behavior of the system with reaction when a fault occurs on h_p, with and without the AO-based FTC.

5.2.2. Sensor fault on T_p

At $t_f = 200\,\text{s}$, a sensor fault $f_{s1} = 4\,^\circ\text{C}$ occurs on the first sensor, *i.e.* the measurement of T_p. Thus, the output of the faulty sensor becomes $y_1^f = y_1 + f_{s1}$. Figure 15 shows the output temperature of the process fluid under different situations: with and without the FTC scheme. After the occurrence of the fault, it is clear that the output of the sensor $T_{p,mea}$ is no longer equal to the output of the system $T_{p,sys}$. However, the proposed FTC scheme allows the output of the system $T_{p,sys}$ to follow the desired temperature $T_{p,d}$ even in the case of a sensor fault.

Therefore, we can conclude that the designed AO-based FTC scheme has the ability to compensate dynamic and sensor faults that may occur on the system with reactions.

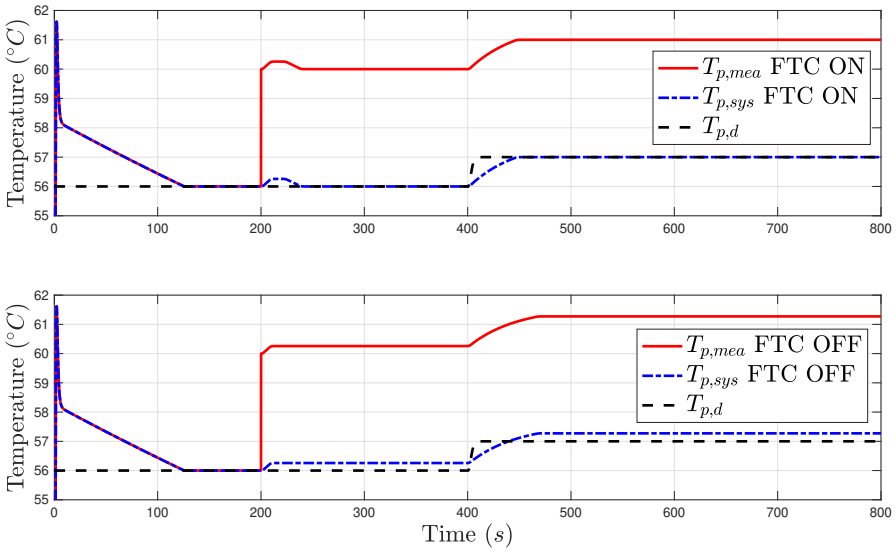

Figure 15: Behavior of the system with reaction when a fault occurs on the sensor of T_p, with and without the AO-based FTC.

6. Conclusion

In this paper, a first work on applying an AFTC system to a specific HEX reactor is presented. The study is divided into two parts: in the first part, we consider the system with only the heat exchange procedure and without the reaction, and in the second one, we add an exothermic reaction. This AFTC system consists of an AO-based FDI method and a nonlinear controller design based on a backstepping approach. The target of this work is to maintain the process fluid temperature of the HEX reactor at the desired value, even in the presence of dynamic faults and sensor faults. Simulation results have proven the efficiency of the AO-based FTC scheme on our HEX reactor system.

In this paper, the system is considered perfect, *i.e.* without noise on sensors and actuators. However, in the practical HEX reactor system, there is always noise. Then, for future work, the AO-based FTC system can be performed on the system with the presence of noise. In addition, a simplified model affected by a single dynamic or sensor fault is considered in this paper. Further studies will focus on the AO-based FTC method for the complicated system with multiple units and multiple fault cases. Moreover, the AO-based FTC method will be tested experimentally on the real HEX reactor pilot.

Acknowledgements

The authors gratefully acknowledge the financial support provided by China Scholarship Council (CSC).

References

[1] A. I. Stankiewicz, J. A. Moulijn, et al., Process intensification: transforming chemical engineering, Chemical engineering progress 96 (1) (2000) 22–34.

[2] J. Etchells, Process intensification: Safety pros and cons, Process Safety and Environmental Protection 83 (2) (2005) 85–89.

[3] D. Reay, C. Ramshaw, A. Harvey, Process Intensification: Engineering for efficiency, sustainability and flexibility, Butterworth-Heinemann, 2013.

[4] Z. Anxionnaz, M. Cabassud, C. Gourdon, P. Tochon, Heat exchanger/reactors (hex reactors): concepts, technologies: state-of-the-art, Chemical Engineering and Processing: Process Intensification 47 (12) (2008) 2029–2050.

[5] F. Theron, Z. Anxionnaz-Minvielle, M. Cabassud, C. Gourdon, P. Tochon, Characterization of the performances of an innovative heat-exchanger/reactor, Chemical Engineering and Processing: Process Intensification 82 (2014) 30–41.

[6] M. Blanke, M. Kinnaert, J. Lunze, M. Staroswiecki, J. Schröder, Diagnosis and fault-tolerant control, Vol. 2, Springer, 2006.

[7] R. Isermann, Fault-diagnosis systems: an introduction from fault detection to fault tolerance, Springer Science & Business Media, 2005.

[8] Z. Gao, C. Cecati, S. X. Ding, A survey of fault diagnosis and fault-tolerant techniques—part i: Fault diagnosis with model-based and signal-based approaches, IEEE transactions on industrial electronics 62 (6) (2015) 3757–3767.

[9] J. Jiang, X. Yu, Fault-tolerant control systems: A comparative study between active and passive approaches, Annual Reviews in control 36 (1) (2012) 60–72.

[10] S. X. Ding, Model-based fault diagnosis techniques: design schemes, algorithms, and tools, Springer Science & Business Media, 2008.

[11] J. Korbicz, J. M. Koscielny, Z. Kowalczuk, W. Cholewa, Fault diagnosis: models, artificial intelligence, applications, Springer Science & Business Media, 2012.

[12] R. J. Patton, P. M. Frank, R. N. Clark, Issues of fault diagnosis for dynamic systems, Springer Science & Business Media, 2013.

[13] S. X. Ding, P. Zhang, T. Jeinsch, E. Ding, P. Engel, W. Gui, A survey of the application of basic data-driven and model-based methods in process monitoring and fault diagnosis, IFAC Proceedings Volumes 44 (1) (2011) 12380–12388.

[14] M. Mansouri, M.-F. Harkat, H. Nounou, M. N. Nounou, Data-driven and model-based methods for fault detection and diagnosis, Elsevier, 2020.

[15] L. Ming, J. Zhao, Review on chemical process fault detection and diagnosis, in: 2017 6th International Symposium on Advanced Control of Industrial Processes (AdCONIP), IEEE, 2017, pp. 457–462.

[16] Q. Jiang, X. Yan, B. Huang, Review and perspectives of data-driven distributed monitoring for industrial plant-wide processes, Industrial & Engineering Chemistry Research 58 (29) (2019) 12899–12912.

[17] J. M. Ali, N. H. Hoang, M. A. Hussain, D. Dochain, Review and classification of recent observers applied in chemical process systems, Computers & Chemical Engineering 76 (2015) 27–41.

[18] O. A. Sotomayor, D. Odloak, Observer-based fault diagnosis in chemical plants, Chemical Engineering Journal 112 (1-3) (2005) 93–108.

[19] E. Bernardi, E. J. Adam, Observer-based fault detection and diagnosis strategy for industrial processes, Journal of the Franklin Institute 357 (14) (2020) 10054–10081.

[20] M. He, Z. Li, X. Han, M. Cabassud, B. Dahhou, Development of a numerical model for a compact intensified heat-exchanger/reactor, Processes 7 (7) (2019) 454.

[21] M. Zhang, B. Dahhou, Q. Wu, Z. Li, Observer based multi-level fault reconstruction for interconnected systems, Entropy 23 (9) (2021) 1102.

[22] M. Zhang, Z. Li, Q.-M. Wu, B. Dahhou, M. Cabassud, Actuator fault diagnose for interconnected system via invertibility, International Journal of Modelling, Identification and Control 33 (4) (2019) 283–298.

[23] M. Zhang, Z. Li, M. Cabassud, B. Dahhou, An integrated fdd approach for an intensified hex/reactor, Journal of Control Science and Engineering 2018 (2018).

[24] M. He, Z. Li, B. Dahhou, M. Cabassud, The fault tolerant control design of an intensified heat-exchanger/reactor using a two-layer, multiple-model structure, Sensors 20 (17) (2020) 4888.

[25] X. Han, Z. Li, M. Cabassud, B. Dahhou, A comparison study of nonlinear state observer design: Application to an intensified heat-exchanger/reactor, in: 2020 28th Mediterranean Conference on Control and Automation (MED), IEEE, 2020, pp. 162–167.

[26] P. V. Kokotovic, The joy of feedback: nonlinear and adaptive, IEEE Control Systems Magazine 12 (3) (1992) 7–17.

[27] L.-P. Xin, B. Yu, L. Zhao, J. Yu, Adaptive fuzzy backstepping control for a two continuous stirred tank reactors process based on dynamic surface control approach, Applied Mathematics and Computation 377 (2020) 125138.

[28] P. Biswas, A. N. Samanta, Backstepping control of polymerization reactor, in: 2013 9th Asian Control Conference (ASCC), IEEE, 2013, pp. 1–5.

[29] P. Kokotović, M. Arcak, Constructive nonlinear control: a historical perspective, Automatica 37 (5) (2001) 637–662.

[30] S. Vaidyanathan, S. Jafari, V.-T. Pham, A. T. Azar, F. E. Alsaadi, A 4-d chaotic hyperjerk system with a hidden attractor, adaptive backstepping control and circuit design, Archives of Control Sciences 28 (2018).

[31] M. K. Shukla, B. B. Sharma, A. T. Azar, Control and synchronization of a fractional order hyperchaotic system via backstepping and active backstepping approach, in: Mathematical Techniques of Fractional Order Systems, Elsevier, 2018, pp. 559–595.